

CONFORMATION OF MONONUCLEOTIDES AND DINUCLEOSIDE MONOPHOSPHATES

P{H} AND H{H} NUCLEAR OVERHAUSER EFFECTS

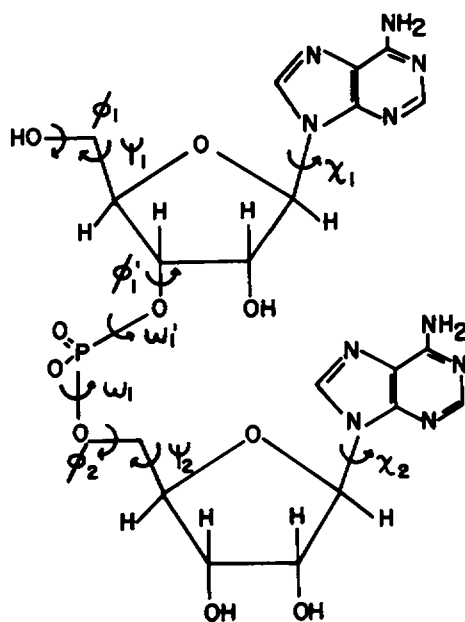
PHILLIP A. HART, *School of Pharmacy, University of Wisconsin,
Madison, Wisconsin 53706 U.S.A.*

ABSTRACT The phosphorus-proton nuclear Overhauser effect (NOE) was used to investigate the quantitative distribution of rotamers about the C3'—O3' bond (ϕ') of 3'-AMP and 2',3'-cyclic-CMP and the C4'—C5', C5'—O5' bonds (ψ , ϕ) of 5'-AMP. Phosphorus-proton and proton-proton NOE's were used to provide a qualitative insight into the backbone conformation and the glycosyl angle torsions of adenosyl-(3' \rightarrow 5')-adenosine (ApA). The major ψ rotamer in 5'-AMP is the 60° (gg) form, while the major ϕ rotamer is the 180° (g'g') form. The constrained model, 2',3'-cyclic-CMP, manifests the C3'-endo furanose pucker predominantly. The results from these two models are consistent with nuclear magnetic resonance (NMR) J coupling analyses. The ϕ' distribution of 3'-AMP is dominated (77%) by the 180° g⁻ rotamer. The 3'-AMP results are consistent with phosphorus-hydrogen coupling constant analyses, but do not accord with phosphorus-carbon coupling constant results. The phosphorus-proton NOE reveals that the phosphorus of ApA occupies a region of conformation space not seen in 5'-AMP. The proton-proton NOE on ApA shows a significant portion of *syn* rotamer in both χ distributions and detects a cross-purine ring interaction consistent with base stacking known to exist in this system.

INTRODUCTION

The objective of present experimental conformational analyses of dinucleoside monophosphates, dinucleotides, and oligonucleotides in solution is to describe the rotamer distribution about the glycosyl bond, the bonds of the furanose ring, and all the bonds of the phosphodiester backbone. Fig. 1 depicts those bonds, labeled conventionally (1), on the framework of the dinucleoside monophosphate adenosyl-(3' \rightarrow 5')-adenosine (ApA), and Table I gives the various conventions used to describe torsion angles referred to them. I intend to establish that these rotamer distributions are a function of pH, temperature, and ionic strength of various electrolytes, and furthermore that the correlations between conformation and the various environmental

This paper was part of the Symposium on Applications of Nuclear Overhauser Effect to Biopolymer Structure, organized by D. W. Urry, held at the Annual Meeting of the Biophysical Society on 26 March 1978.



ApA

FIGURE 1 Structure and torsion angles of adenosyl-(3' → 5')-adenosine (ApA). The structure is partitioned into two parts for easy reference: the Ap or 3'-nucleotide part and the pA or 5'-nucleotide part. See Fig. 2 for the numbering scheme.

TABLE I
TORSION ANGLE CONVENTIONS

Angle	Atom basis	Some specific designations		
ϕ'	P3'—O3'—C3'—C4'	60°	180°	-60°*
	P3'—O3'—C3'—C4'	g^+	t	g^-
	P3'—O3'—C3'—H3'	t	g^-	g^+
ψ	O5'—C5'—C4'—C3'	60°	180°	-60°
	O5'—C5'—C4'—C3'	g^+	g	g^-
	H5',5''—C5'—C4'—H4'	gg	gt	tg
ϕ	P5'—O5'—C5'—C4'	180°	-60°	60°
	P5'—O5'—C5'—C4'	t	g^-	g^+
	P5'—O5'—C5'—H5',5''	$g'g'$	$t'g'$	$g't'$
χ	O4'—C1'—N9—C4 (purines)	-120°	anti	60°
	O4'—C1'—N1—C2 (pyrimidines)			

*The convention for determining a numerical dihedral angle designation is given in Sundaralingam et al. (1). The numerical designations are far more versatile than the *gauche-trans* nomenclature, but the qualitative designations are so commonly used they are shown as well.

†Illustrated in Fig. 2.

TABLE II
SUMMARY OF TORSION ANGLE DETERMINATIONS FOR
ApA IN AQUEOUS SOLUTION

Torsion angle	Method	Rotamer distribution†							Reference
		-120°	±37°	g ⁻	g ⁺	t	gg	g'g'	
				%					
χ	NMR	100‡							2
φ ₁	³ J _{P,H3'}		100						2
				71§					22
	³ J _{P,C2',C4'}			43	20	37			4
ψ ₂	³ J _{H4',H5',5''}						79		2
							88		22
φ ₂	³ J _{P,H5',5''}							90	2

*φ₁ is referred to P—O3'—C3'—H3'; φ₂ is referred to P—O5'—C5'—H5',5''; ψ₂ is referred to H5',5''—C5'—C4'—H4'.

‡Assumed from monomer studies, not determined directly for dimer. The atom basis for this angle is shown in Table I and the extreme *anti* and *syn* forms are depicted in Fig. 2.

§The g⁺ rotamer is not excluded. It was assumed absent on other grounds.

parameters serve as input to other studies (theoretical calculations for example) potentially able to describe polymeric systems whose complexity exceeds the capability of the methods currently available to fix individual torsion angles (nuclear magnetic resonance [NMR]).

A large body of work reports experimental probes of most of the torsion angles of Fig. 1. This work is too extensive to quote here; Lee et al. (2, 3) and Alderfer and Ts'o (4) have summarized most of it. Table II contains the salient conclusions from this body of work, emphasizing those torsion angles that have been difficult to establish. The summary of Table II is biased toward solution studies and, more specifically, toward NMR *J* coupling analyses because that has been the most commonly applied method. The table is further constrained to a summary of results on ApA, because that model amply illustrates the direction further work should take.

It is apparent from Table II that the most elusive torsion angles are φ', ω, ω', and χ. NMR coupling constant analyses of φ' are either ambiguous or do not agree; there are no direct methods for the determination of ω and ω', and the proton-proton nuclear Overhauser effect (NOE) method, applied successfully to the observation of χ in mononucleosides (5) and mononucleotides (6, 7), has not previously been applied to the more complex systems. Thus, I have initiated a program to extend the homonuclear proton NOE to the determination of χ in dinucleotides and to apply the phosphorus-proton NOE to the determination of φ' and other backbone torsion angles as well in the same systems. Described here are experiments that establish the validity of the phosphorus-proton NOE for the determination of φ' as well as ψ, φ jointly in the mononucleotides 2',3'-cyclic CMP, 3'-AMP and 5'-AMP (Fig. 2). In addition, P{H} and H{H}NOE data on ApA illustrate the potential of these two

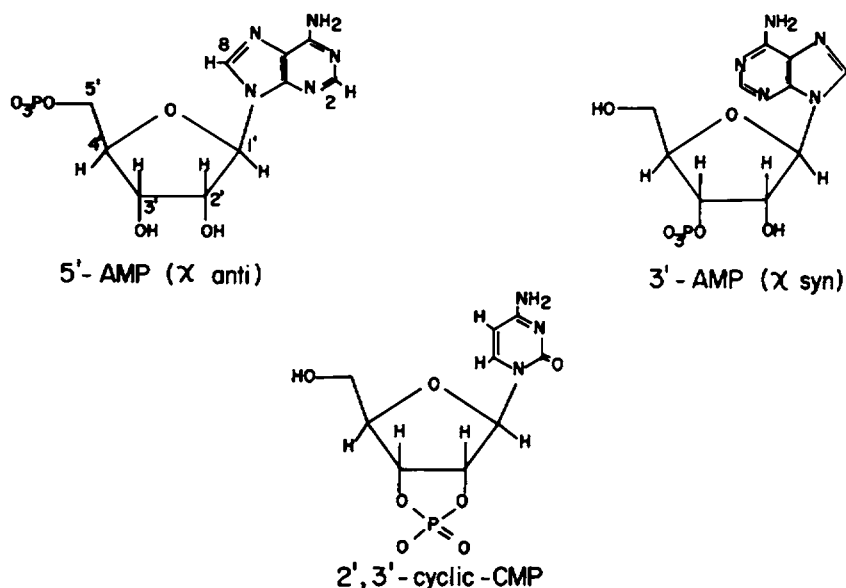


FIGURE 2 Structures of the mononucleotides studied. The extreme *syn* and *anti* forms of the glycosyl torsion angle (χ) are illustrated with 3'- and 5' AMP, respectively.

types of NMR measurement for the conformational analysis of dinucleotides and (perhaps) higher oligonucleotides.¹

THEORY AND ASSUMPTIONS

Noggle and Schirmer (8) have shown that the fractional change of the integrated intensity of nucleus *d* (half-spin, magnetogyric ratio γ_d), when the nuclei *s* (all half-spin, all having the same magnetogyric ratio γ_s) are successively saturated, can be written

$$f_d(s) = \left[\frac{\gamma_s}{2\gamma_d} \sum_s \rho_{ds} - \frac{\gamma_n}{2\gamma_d} \sum_{n \neq d,s} \rho_{dn} f_n(s) \right] / R_d, \quad (1)$$

in which $\rho_{ds} = \gamma_d^2 \gamma_s^2 \hbar^2 \tau_c / r_{ds}^6$ (the dipolar relaxation rate of *d* owing to the single spin *s*); and $R_d = \sum_k \rho_{dk} + \rho_d^*$ (the total relaxation rate of *d*). In these expressions ρ_d^* is the spin-lattice relaxation rate of *d* contributed by independent relaxation mechanisms other than dipole-dipole interactions, τ_c is the time constant for overall molecular reorientation, and r_{ds} is the distance between *d* and *s* in Angstrom units. The definition of $f_n(s)$ appearing in Eq. 1 is entirely analogous to $f_d(s)$. Eq. 1 is a general expression for the NOE in multi-spin systems, given the following assumptions: (a) The extreme narrowing condition is satisfied, that is, $\omega_0 \tau_c \ll 1$ when ω_0 is

¹This compact double-irradiation symbolism is conventional. The bracketed nucleus is irradiated and the unbracketed nucleus is observed.

the Larmor frequency of the nucleus having the larger magnetogyric ratio. (b) All spins are loosely coupled, that is, $J < \Delta\delta$. (c) All dipole-dipole interactions involving the nucleus d are modulated by the same correlation time, τ_c . (d) Other relaxation mechanisms comprising ρ_d^* are characterized by the same correlation time that modulates the dipolar interactions.

While Eq. 1 and modifications of it have been used to effect nucleoside conformational analysis via the $\text{H}\{\text{H}\}$ NOE (5), the equation is sufficiently general to include half-spin nuclei other than that of hydrogen. Indeed, Eq. 1 takes exactly the same form if one heteroatom (say ^{31}P) interacts with other atoms, all of the same nuclear type (say ^1H). In that case, when $\rho^* = 0$ and the extreme narrowing condition is satisfied, $f_p(\text{H}) = \gamma_{\text{H}}/2\gamma_{\text{P}} = 1.24^2$ and this maximum enhancement will be found in a multi-spin system when all hydrogens that can relax the ^{31}P nucleus via dipolar coupling are saturated. If the conditions $\rho^* = 0$ and $\omega_0\tau_c \ll 1$ are not met, the maximum observable $\text{P}\{\text{H}\}$ NOE will be attenuated. It will become apparent later that the most convenient way to account for the incursion of other relaxation mechanisms and violation of the extreme narrowing condition is to modify Eq. 1 to read

$$f_d(s) = \Phi(\omega_d, \omega_s, \tau_c) \frac{1}{\beta} \left[\frac{\gamma_s}{\gamma_d} \sum_s \rho_{ds} - \frac{\gamma_n}{\gamma_d} \sum_{n \neq d, s} \rho_{dn} f_n(s) \right] / R_d^{dd} \quad (2)$$

where

$$\Phi(\omega_d, \omega_s, \tau_c) = \frac{6[1 + (\omega_d + \omega_s)^2\tau_c^2]^{-1} - [1 + (\omega_d - \omega_s)^2\tau_c^2]^{-1}}{6[1 + (\omega_d + \omega_s)^2\tau_c^2]^{-1} + [1 + (\omega_d - \omega_s)^2\tau_c^2]^{-1} + 3[1 + \omega_d^2\tau_c^2]^{-1}},$$

and R_d^{dd} , the total dipolar relaxation rate of d , and β are defined as follows: $R_d^{dd} \equiv R_d - \rho_d^*$; $\beta \equiv R_d/R_d^{dd}$. By measuring the total $\text{P}\{\text{H}\}$ NOE via saturation of all interacting protons, the combined effects of failure of extreme narrowing and other relaxation mechanisms can be discerned. Independent determinations of these separate effects may be obtained from the NOE and T_1 measurements at different magnetic field strengths. It is important to note that the extent to which these effects do depress the observed NOE need not complicate the analysis of these measurements to obtain structural information.

If the assumption that a single τ_c modulates all contributions to the spin-lattice relaxation is maintained, so that ρ^* and the effects of violation of extreme narrowing can be factored as shown in Eq. 2, then τ_c can be eliminated from the expressions for ρ_d^{dd} and the NOE will depend only on r_d^{-6} plus various fixed coefficients. If, further, internal motion is present, with a characteristic frequency much faster than $1/T_1$, the effect of multiple conformations on the measured $f_d(s)$ will be the average of r_d^{-6} over the various weighted conformations. Eq. 2 then takes the form

²It is noted that $f_{\text{H}}(\text{P}) \cong 0.2$, which may be large enough to be useful in special cases; however, it will not be considered further here.

$$f_d(s) = \Phi(\omega_d, \omega_s, \tau_c) \left[\frac{1}{\beta} \left[\frac{\gamma_s}{\gamma_d} \sum_s \langle \gamma_d^2 \gamma_s^2 r_{ds}^{-6} \rangle - \frac{\gamma_n}{\gamma_d} \sum_{n \neq d, s} \langle \gamma_d^2 \gamma_n^2 r_{dn}^{-6} \rangle f_n(s) \right] \right] / R_d^{dd} \quad (3)$$

where $R_d^{dd} = \sum_k \langle \gamma_d^2 \gamma_k^2 r_{dk}^{-6} \rangle$. The average of r^{-6} over the various conformations is used because the observed spin samples all of conformation space many times during one T_1 . A detailed treatment of the rationale for Eq. 3 is given in Noggle and Schirmer (8).

The details of how Eq. 3 may be used to solve the specific conformation problems under present consideration are covered in the Methods section; however, at this point it is appropriate to examine the consequences of the breakdown of the assumption that a single τ_c modulates the dipolar interactions. Multiple correlation times will arise when the overall motion is anisotropic or when internal motion is superimposed upon overall motion. These situations have been studied by Woessner (9, 10), Doddrell et al. (11), Werbelow (12), and Rowan et al. (13). It is either an explicit outcome of, or a conclusion from these studies that when the extreme narrowing condition is satisfied with respect to the correlation time of overall rotation, the NOE is independent of all correlation times.³

A generalized conclusion from the above work is that when τ_c becomes sufficiently large so that the extreme narrowing condition is violated at a given field value, internal motion either can have no effect on or can increase the NOE over what it would be in the absence of internal motion. However, it is clear from the work of Doddrell et al. (11) and Werbelow (12) that, since τ_c and molecular weight are directly proportional, solutes with actual or apparent molecular weights less than 1,000 can be assumed (at 21 kG) to have sufficiently short correlation times for overall motion so that internal motion will have no effect on measured NOE's within experimental error.

METHODS

Sample Preparation

The mononucleotides 3' and 5'-AMP⁴ and the cyclic nucleotide 2',3'-cCMP were purchased from Calbiochem (San Diego, Calif.). The dinucleoside monophosphate ApA was purchased from Boehringer-Mannheim Biochemicals (Indianapolis, Ind.). In general, 0.2 mmol of the samples was dissolved in 2 ml of water and the pH was adjusted to ~8 with sodium hydroxide. The samples were successively lyophilized as frozen solutions in water 99.8% D₂O and "100%" D₂O. The final dry residues were taken up in ~1 ml of "100%" D₂O and the resultant solutions were passed through 1-2 cm columns of Chelex 100 (Bio-Rad Laboratories, Richmond, Calif.) previously equilibrated with "100%" D₂O. The columns were washed with the same solvent and the wash eluent was used to dilute the samples to a final concentration of 0.1 M. Final pH measurements were made at this stage because pH is generally increased by the Chelex treatment.⁵ The samples were sparged with argon, then transferred (with minimum exposure

³Unpublished work of C. F. Anderson.

⁴Abbreviations used in this paper: AMP, adenosine monophosphate; ApA, adenylyl (3' → 5') adenosine; cCMP, cyclic cytidine monophosphate; EDTA, ethylenediamine tetraacetic acid; NMR, nuclear magnetic resonance; NOE, nuclear Overhauser effect.

⁵All reported values of this work have been corrected for the deuterium isotope effect by adding 0.4 to the pH meter reading.

to oxygen) to 10-mm cylindrical inserts (Wilma Glass Co., Inc., Buena, N.J.) of a configuration that constrained the sample within the dimensions of the spectrometer receiver coil. While nearly any sample configuration is satisfactory for NOE measurements, these samples were to be used in an extensive series of ^{31}P T_1 measurements requiring the constrained sample configuration. All glassware that was to contact the samples after Chelex treatment was rinsed with basic EDTA, deionized water, and acetone, blown dry, and then flamed until nearly incandescent. The ApA sample for $\text{H}\{\text{H}\}$ experiments was transferred to a 5-mm tube, sparged with argon, and then degassed via three freeze-thaw cycles at 10^{-5} Torr; then the tube was sealed.

NOE Measurements

NMR measurements were made with a Bruker HX90E spectrometer modified for quadrature detection (^2H lock) (Bruker Instruments, Inc., Billerica, Mass.). Phosphorus resonance was observed at nominal 36.44 MHz and proton resonance at 90 MHz. Generally, an observing pulse of $30\text{--}40^\circ$ was used and the delay was determined empirically for maximum signal intensity. Free induction decays were collected into and Fourier transformed by a Nicolet 1080 computer (Nicolet Instrument Corp., Madison, Wis.) Exponential multipliers resulting in 0.25 Hz broadening were applied and digital resolution was 0.25 Hz.

An unperturbed phosphorus spectrum was first collected (200 transients); then the perturbed spectrum was measured with the proton decoupler at a single frequency (low power) or a broad band of frequencies (high power). Signal areas were measured on expanded spectra via planimetry, and area differences between the perturbed and the unperturbed spectra were recorded as positive or negative NOE's expressed as percentage change. If the signal-to-noise ratio was greater than 20/1, actual experimental precision was 5%. Decoupling power in the low-power experiments was ~ 1 mG, measured according to Leigh (14). Probe temperature was $25^\circ\text{C} \pm 0.1^\circ\text{C}$.

Computation and Fitting

Bond lengths and angles for 2',3'-cCMP are those reported for the A form by Coulter (15), those for 3'-AMP were reported by Sundaralingam (16), and those for 5'-AMP were reported by Kraut and Jensen (17). These solid-state structural parameters were entered into a general BASIC program for computation of relevant internuclear distances by the Nicolet 1080. The geometry program locates a predetermined atom at the origin of a Cartesian coordinate system, then transforms the internal geometry (molecular-centered) of successive defined atoms to the Cartesian coordinate system. This method is discussed in somewhat greater detail by White (18). The program uses dihedral angles as variable input and it assumes that bond lengths and angles remain constant under conformational change. The distances are raised to the -6 power and averaged over all predetermined conformations, and the averages are entered into as many equations of the type of Eq. 2 as are prescribed by the model (16 for cCMP and 3'-AMP, 8 for 5'-AMP); the sets of simultaneous equations are solved iteratively. The resultant computed enhancements are reduced by the ratio of total NOE to theoretical NOE (as discussed in the Theory section) and also by an estimated factor that corrects for the NOE incompletely developed because of lower than optimum proton irradiation power. It has been shown (19) that irradiation of a proton singlet at the 1 mG level results in enhancements of proximate nuclei 10% below the maximum attainable values. In the present work, multiplets were irradiated at the 1 mG level, and because more irradiation power is required to saturate a multiplet than is required for a singlet, the correction of the computed enhancements for incomplete saturation was chosen to be 0.8. That is, all observed enhancements were assumed to be 20% lower than would be observed if proton chemical shift dispersion were great enough to permit complete saturation of individual proton resonances. The corrected computed enhance-

ments were then compared visually with their experimental counterparts and the process was repeated until similar profiles were achieved. No unreasonable conformations (based on inspection of Prentice-Hall framework molecular models, Prentice-Hall, Inc., Englewood Cliffs, N.J.) were tested and the final conformations did not show excessive van der Waals contacts. Presently, neither a high resolution search of dihedral angles nor a bond length and bond angle optimization was possible. High-speed computation will be required for that work.

Spectral Assignments

The proton spectra of all the nucleotides considered in the present work have been thoroughly studied and documented. 2',3'-cCMP was reported by Lavalée and Coulter (20) and by Lapper and Smith (21). The remaining nucleotides are summarized by Lee et al (2, 3).

RESULTS AND DISCUSSION

Experimental enhancements and computed enhancements corresponding to the best-fit conformations are recorded for 2',3'-cCMP, 3'-AMP, and 5'-AMP in Tables III, IV, and VI. Preliminary phosphorus-proton and proton-proton NOE data for ApA are recorded in Table VIII. The recorded best-fit conformations are specified by a single best value for each angle in the relevant conformation space. Although there must be a distribution of finite width about the value cited for each angle, the present analysis can provide no information about such distributions. The ensuing discussion illuminates those findings that can be stated with reasonable certainty. Further extensive computation will probably refine the torsion angle positions and their relative proportions, but it is unlikely that the general sense of the conclusions will be altered.

cCMP

The NOE data of Table III confirm the expected spatial interaction of the phosphorus and H-1',2',3', and 4' in this moderately constrained system. The computed enhancement profile, reasonably congruent with the experimental profile, is derived from a

TABLE III
EXPERIMENTAL ENHANCEMENTS AND BEST-FIT CONFORMATION
DISTRIBUTION 2',3'-CYCLIC CMP*

Proton(s) irradiated	Observed enhancement†	Best-fit computed enhancement (corrected)	Best-fit conformations‡		
			Sugar	ϕ'	%
All	0.80				
1'	0.09	0.09	C3' endo	125°	85
2'	0.15	0.12	C2' endo	150°	15
3'	0.12	0.11			
4'	0.16	0.15			
5',5''	0.01	-0.02			

*0.1 M solution. pD = 7.2.

†30° pulse, 15-s delay, 200 transients.

‡Hydroxymethylene side chain 0.35:0.46:0.19 gg:gt:tg.

0.85:0.15 C3'endo:C2'endo sugar conformation and two different puckered conformers of the cyclic phosphate. The two cyclic phosphate conformers are envelope forms, in which one of the oxygens is below the plane of the other four atoms. This out-of-plane atom will be designated *exo*, in keeping with standard nucleotide nomenclature. The sugar and cyclic phosphate conformers are allowed to occur simultaneously so that the O2' *exo* cyclic phosphate conformer corresponds to the C3' *endo* sugar conformer and the O3' *exo* cyclic phosphate corresponds to the C2' *endo* sugar. The computations allow the exocyclic hydroxymethylene group to assume a 0.35:0.46:0.19 *gg:gt:tg* distribution as determined by Lapper and Smith (21); however, the nature of this distribution has a negligible influence on the computed enhancement profile. The NOE-derived conformation agrees qualitatively with that determined from NMR coupling constants by Lavalley and Coulter (20) and by Lapper and Smith (21). The coupling constant analyses gave the qualitative result that pyrimidine 2',3' cyclic phosphate manifested a preference for the C3' *endo* sugar; it was not possible to define the C3' *endo*, C2' *endo* ratio, nor the status of the cyclic phosphate via the coupling constant analyses. Neither NMR method affords a solution conformation like the solid-state structure determined by Coulter (15). The crystal manifests a nearly planar furanose ring.

The outer lines of the H2' and H3' multiplets overlap at 21 kG and, as a result, neither proton multiplet can be saturated independently. Additionally, δ/J for the 2',3' protons is 2.8, a value in violation of the weak-coupling limit of 10 suggested by Noggle and Schirmer (8). Violation of the weak-coupling limit introduces errors in the H{H} NOE's and this error is transferred to the P{H} NOE's via the second term of Eq. 2. As that term is usually small, the errors are probably negligible at the present level of the analysis. Multiple irradiation can, however, introduce uncertainties that cannot be ignored. In the present case, it is likely that the phosphorus enhancement due to H2' irradiation is too large because some of the H3' effect is included and that the P-H3' interaction is overestimated because some of the H2' effect is included. In contrast, H1' and H4' can be saturated independently from each other and from other protons as well. Because the data from the H1',4' irradiations are more accurate than those from the H2',3' irradiations, greater effort was made to "fit" the computed H1',4' enhancements to their experimental counterparts than was made in the H2',3' case. It is not understood why no small negative experimental P{H5',5''} effect is observed (see Table III). The important outcome of the above experiments on cCMP is that the P{H} NOE method has located the phosphorus in an altogether reasonable region of conformation space.

3'-AMP

The NOE profile recorded in Table IV for 3'-AMP gives qualitative evidence for at least two ϕ' conformation ranges. The P{H4'} effect and the negative P{H5',5''} effect are suggestive of the 60° (P,O3',C3',H3' *trans*) rotamer; the large P{H2'3'} effect is equivocal; however, in the absence of a positive P{H5',5''} effect, it suggests a 180° (*g-*) rotamer. These inferences are supported by the computations. The com-

TABLE IV
EXPERIMENTAL ENHANCEMENTS AND BEST-FIT CONFORMATION
DISTRIBUTION 3'-AMP*

Proton(s) irradiated	Observed enhancement†	Best-fit computed enhancement (corrected)	Best-fit conformations		
			ϕ'	C3':C2' Endo	%
all	0.95				
1'	0.025	0.012	180°	0.36:0.64	77
2' + 3'	0.34	0.42	60°	1:0	23
4'	0.15	0.20			
5',5''	-0.065	-0.02			

*0.1 M solution; pD = 9.9.

†30° pulse, 15-s delay, 200 transients.

putations were made under the assumption of Lee et al. (2) that the 60° (t) rotamer is not favored on steric grounds. Steric strain is discernible upon examination of molecular models and arises from the H1',H4', phosphate interaction when the furanose assumes the C2' endo conformation. Steric compression appears to be substantially relieved when the furanose assumes the C3' endo conformation; therefore in the computations, the 60° rotamer was allowed to occur jointly only with the C3' endo sugar pucker. The computed ϕ' distribution is therefore, 77% of the 180° (g-) rotamer superimposed upon a 36:64 C3' endo:C2' endo sugar equilibrium plus 23% of the 60° (t) rotamer superimposed upon a pure C3' endo sugar pucker. The -60° (gt) rotamer is precluded because that rotamer requires a moderate positive P{H5',5''} enhancement regardless of the sugar conformation. It is suggested by the above results that the sugar conformation and ϕ' angle do not vary independently.

Are the above conclusions consistent with the findings of three-bond phosphorus-hydrogen and phosphorus-carbon coupling constant analyses summarized in Table VII? The three-bond coupling of P3' and H3' will not distinguish between the 180° (g-) and the -60° (g+) ϕ' rotamers. Cozzone and Jardetsky (22) have concluded from their $^3J_{P,H3'}$ values that the g- and/or g+ rotamers represent 67% of the ϕ' distribution at pH 3 and 76% at pH 11. They conclude further that the g- isomer is preferred, because of chemical shift evidence for a phosphate - 2'OH interaction at higher pH. On the other hand, Lee et al. (2) conclude from their $^3J_{P,H3'}$ values that the ϕ' conformation is exclusively the + or - 37° P,O3',C3',H3'-based rotamer. Phosphorus-carbon three-bond coupling constants ($^3J_{P,C2'}$ and $^3J_{P,C4'}$) indicate a major (70%) contribution by the 60° (t) rotamer to the ϕ' distribution (23). It is not clear why the phosphorus-carbon and the phosphorus-proton vicinal coupling constant analyses are disparate. Table V presents computed enhancements corresponding to the three coupling-constant-derived ϕ' distributions to demonstrate that the NOE method can distinguish among them. It is apparent that the Cozzone and Jardetsky (22) conformation is supported by the NOE analysis.

TABLE V
COMPUTED ENHANCEMENTS FOR THREE COUPLING-CONSTANT-DERIVED
ROTAMER DISTRIBUTIONS OF 3'-AMP

ϕ	C3' endo:C2' endo	Uncorrected enhancements				
		fP(1')	fP(2')	fP(3')	fP(4')	fP(5',5'')
-157*	0.36:0.64	0.02	0.10	0.91	0.05	0.006
-83‡	0.36:0.64	0.01	0.01	0.77	0.16	0.05
60° } 180° }	0.7:0.3	0.34	0	0.25	0.33	-0.05

*Corresponds to the -36° rotamer of Lee et al. (2).

‡Corresponds to the +36° rotamer of Lee et al. (2).

5'-AMP

The NOE-derived best-fit ψ , ϕ distributions of Table VI accord fairly well with distributions derived from both phosphorus-hydrogen and phosphorus-carbon coupling constants (Table VII). There are, however, subtle differences in the distributions revealed by the three methods, which must be discussed before valid comparisons can be made. Phosphorus-proton three-bond coupling constants provide a measure of rotamer probabilities about the individual bonds ψ and ϕ . These measurements say nothing about joint probabilities of the ψ , ϕ pair. The 5'-AMP coupling constant analyses shown in Table VI reveal a high separate probability of finding ψ in the 60° (gg) range and of finding ϕ in the 180° (g'g') range. Unconditional joint probabilities, $P(\psi \cap \phi)$, are obtained by multiplying the individual experimental probabilities of Table VII. The phosphorus-carbon three-bond coupling constant of 5'-AMP reflects the status of the O5'-C5' bond (ϕ) only and is consistent with the phosphorus-proton results in suggesting a high proportion of the 180° (g'g') rotamer.

Four-bond phosphorus-hydrogen coupling constants reflect the joint distribution

TABLE VI
EXPERIMENTAL ENHANCEMENTS AND BEST-FIT CONFORMATION
DISTRIBUTION 5'-AMP*

Proton(s) irradiated	Observed enhancement‡	Best-fit computed enhancement (corrected)	Best-fit conformation§		
			ψ (deg)	ϕ (deg)	%
all	1.07				
3'	small	.012	60	180	72
4'	0.14	.16	-60	-60	14
5',5''	0.47	.54	60	-60	14

*0.1 M solution. pD = 8.5.

‡30° pulse, 15-s delay, 200 transients.

§C3' endo:C2' endo 0.36:0.64.

|| Actual enhancement ~0.02; however, this might be result of overlap with H4'.

TABLE VII
SUMMARY OF PUBLISHED COUPLING CONSTANT ANALYSES
FOR 3' AND 5' AMP

Compound	Coupling constant	Estimated conformation distribution			P($\psi \cap \phi$)	Reference
		ϕ'	ψ	ϕ		
		$\pm 36^\circ$ g ⁻ t	gg	g'g'		
3'-AMP	$^3J_{P,H3'}$	100 (pD 5.4)				2
		67 (pH 3)				22
		76 (pH 11)				22
5'-AMP	$^3J_{P,C2',C4'}$	30 70				23
	$^3J_{H4',H5',5''}$		77 (pD 5.4)			2
	$^3J_{P,H5',5''}$			72 (pD 5.4)	0.55	2
				85		22
	$^3J_{P,C4'}$			80		23
	$^4J_{P,H4'}$		High proportion gg, g'g'			25, 26

ϕ' is referred to P,O3',C3',H3', ψ is referred to H5',5'',C5',C4',H4' and ϕ is referred to P5',O5',C5',H5',5''.

about *two* intervening bonds, the ψ , ϕ joint distribution in the present case. Based on the earlier work of Hall and Malcolm (24), Evans and Sarma (25) and Sarma et al. (26) have concluded that the $^4J_{P,H4'}$ (~ 2 Hz) observed for the 5'-nucleotides corresponds to a coplanar W arrangement of P,O5',C5',C4',H4', an arrangement that corresponds to the 60°, 180° (gg, g'g') joint ψ , ϕ distribution. Because of the difficulty of accurately measuring coupling constants in the 0–2-Hz range and because the complete torsion angle (joint in this case) dependence of $^4J_{P,H}$ is unknown, this coupling constant can be used as a qualitative indicator only; nevertheless, it is, as will be shown below, a valuable one.

The phosphorus-proton NOE is also a direct reflection of the ψ , ϕ joint distribution and the experimental enhancements correspond to a computed joint ψ , ϕ probability that is 0.72 gg, g'g'. The NOE-derived value is in fair agreement with the value computed from the phosphorus-proton coupling constant results (Table VII). To compare the NOE results with the phosphorus-carbon and phosphorus-hydrogen coupling constant results it is necessary to assume that $(0.72)^{1/2}$ is the NOE-derived ϕ rotamer probability. That value, 0.85, compares favorably with the value (0.8) from the phosphorus-carbon data (22) and with the value (0.85) from the phosphorus-hydrogen data (21), but the agreement may be fortuitous.

Another distribution of conformations of the phosphate side chain of 5'-AMP yields computed enhancements that correspond fairly well with the experimental set. The major conformer of this new distribution retains the *trans* P,O5',C5',C4' arrangement; however, the ψ angle is in the 180° (gt) region. This distribution can probably be discounted however, because changing ψ from 60° to 180° causes a significant deviation from the coplanar W arrangement of P,O5',C5',C4',H4' responsible for the observed $^4J_{P,H4'}$ of 2 Hz. As expected, the computed ψ , ϕ distribution is independent of the furanose C3' endo, C2' endo ratio.

TABLE VIII
PHOSPHORUS-PROTON AND PROTON-PROTON NOE DATA FOR
ADENOSYLYL-(3' → 5')-ADENOSINE

Proton(s) irradiated	Phosphorus enhancement	Proton enhancements*			
		ApH8	pAH8	ApH2	pAH2
All	0.78				
Ap1'	0	0.13	0	-0.01	0.036
pA1'	0	0.23	0.16	0.07	0.02
pA2',3'	0.20	0	0.13	0	0.03
Ap2',3'	0.30	0.10	0.14	0.02	0.03
Ap5',5''	0.01				
Ap4'; pA4',5',5''	0.32				

*Saturating field applied for 2 s before and turned off during FID accumulation.

It therefore appears that all conformational analyses of the phosphate side-chain of 5'-AMP lead to a similar conformation distribution. The observed differences may be due to differences in pD. Future work will address the question of conformation dependence on pD.

ApA

The phosphorus-proton and proton-proton NOE data recorded in Table VIII have not been analyzed quantitatively; nonetheless it is possible to apply conformation indicators developed in simpler systems to this more complex example. The NOE experiments probe two regions of the dinucleoside directly, namely the phosphodiester backbone and the glycosyl bond. As well, they might eventually provide (see below) indirect evidence for certain arrangements of the immediate phosphodiester bonds ω and ω' .

THE PHOSPHODIESTER BACKBONE Despite inadequate chemical shift dispersion at 21 kG it is possible to saturate selectively those regions indicated in the table. The effects seen when ApH2',3' and pAH5',4'-APH4' are irradiated are unexceptional because those protons are immediately adjacent to the phosphorus for most backbone conformations. The negligible effect seen on irradiation of ApH5',5'' (definitely not negative) indicates that the ϕ'_1 distribution contains very little of the g+ rotamer and that it may contain none of the t rotamer. The substantial effect seen on irradiation of pAH2',3', unexpected on the basis of the 5'-AMP results, was verified at lower power to avoid irradiation of other resonances. This enhancement points to the occupation of a new region of conformation space by the phosphorus. This new region is probably characterized by a P-pAH3' interaction rather than a P-pAH2' interaction, because molecular models suggest the latter interaction would be unlikely.

To accomplish more selective proton irradiation it will be necessary to effect various permutations of deuterium substitution at Ap4',5',5'' and pA4',5',5''. Such extensive substitution would not be required if it were possible to conduct the P{H} NOE experiments at, for example, 63 kG; however at higher fields, modulation of the anisot-

ropy of the phosphorus chemical shift may become a dominant relaxation pathway, and if that were the case the NOE's would be substantially reduced. Deuterium substitutions are in progress and will allow the determination of ϕ'_1 , ψ_2 , and ϕ_2 analogously to the mononucleotide analyses.

GLYCOSYL TORSION ANGLES The proton-proton NOE data presented in Table VIII afford qualitative information about the glycosyl torsion angles of both monomer units of ApA. The substantial ApH8 {ApH1'} and pAH8 {pAH1'} enhancements are clear indicators that *syn* rotamers ($\chi = -120^\circ$) compose some proportion of each glycosyl bond rotamer distribution. Indeed, past work on monomeric species (5-7, 27) indicates that proportion could be 0.5 or greater. The 1' resonances are 12 Hz apart at 21 kG and are well-separated from other regions of the ApA proton spectrum; thus the ApH8 and pAH8 enhancements are uniquely associated with the ApH1' and pAH1' irradiations.

Consistent with the results of H1' irradiations are the results of ApH2',3' and pAH2',3' irradiations. These experiments probe the *anti* glycosyl region ($\chi = 60^\circ$); the substantial H8 enhancements seen as a result of these experiments indicate that the *anti* regions are populated as well. The H2',3' irradiations will not be quantifiable, however, until it becomes possible to irradiate the two sugar protons separately. That can be accomplished for pAH2',3' by working at a 63 kG field strength, at which the two protons are adequately separated. Selective deuterium substitution will be required for the ApH2',3' region because those protons overlap completely even at 63 kG.

The proton-proton NOE data that are particularly intriguing are the ApH8 {pAH1'} and the pAH8 {ApH2',3'} enhancements. Those data indicate interactions *between* the Ap and the pA units. These cross-interactions are consistent with base-stacking interactions typical of purine dinucleoside monophosphates; thus, the NOE experiments may eventually provide another means of quantifying that interaction directly. Furthermore, if it is possible to gauge cross-monomer unit interactions, it may be possible, in conjunction with ψ , ϕ , ϕ' analyses, to arrive at an indirect assessment of the ω , ω' populations.

Summary

The foregoing demonstrates that phosphorus-proton and proton-proton nuclear Overhauser effect measurements are useful tools for nucleotide and dinucleotide conformational analysis. For example, the phosphorus-proton experiment allows a clear choice between the -60° and 180° ϕ' rotamers and allows the detection and quantification of minor ψ , ϕ rotamers. The proton-proton experiment allows a determination of the *syn-anti* χ distribution. These distinctions are difficult or impossible to make by other methods. The ApA results give a strong indication that the methods can be applied to more complex systems. An objective means of correcting for partial saturation is needed because small errors are very likely introduced by the current practice of making uniform corrections. That means is being sought.

I thank Dr. Charles F. Anderson for many helpful discussions, in particular those related to the effects of internal motion on the NOE. I am grateful to Professor Gordon Amidon for supplying a FORTRAN

version of the geometry program and to Professor M. P. Klein for suggesting the means of measuring H_2 field strength. James Blackburn provided technical assistance.

Funds were provided by a National Institutes of Health Biomedical Research Support Grant (1 SO7 RR-05456) and from National Science Foundation grant PCM77-19927.

Received for publication 16 May 1978 and in revised form 22 July 1978.

REFERENCES

1. SUNDARALINGAM, M., B. PULLMAN, W. SAENGER, V. SASISEKHARAN, and H. R. WILSON. 1973. Recommendations of standard conventions and nomenclature for the description of the conformation of polynucleotide chains. In *Conformations of Biological Molecules and Polymers. Jerus. Symp. Quantum Chem. Biochem.* 5:815.
2. LEE, C.-H., F. S. EZRA, N. S. KONDO, R. H. SARMA, and S. S. DANYLUK. 1976. Conformational properties of dinucleoside monophosphates in solution: dipurines and dipyrimidines. *Biochemistry*. 15: 3627.
3. LEE, C.-H., and I. TINOCO, JR. 1977. Studies of the conformation of dinucleoside phosphates containing I, N⁶-ethenoadenosine and 2'-O-methylcytidine by 360 MHz ¹H nuclear magnetic resonance spectroscopy. Investigation of the conformation of dinucleoside phosphates. *Biochemistry*. 16:5403.
4. ALDERFER, J. L., and P. O. P. TS'0. 1977. Conformational properties of the furanose phosphate backbone in nucleic acids. A carbon-13 nuclear magnetic resonance study. *Biochemistry*. 16:2410.
5. SCHIRMER, R. E., J. P. DAVIS, J. H. NOGGLE, and P. A. HART. 1972. Conformational analysis of nucleosides in solution by quantitative application of the nuclear Overhauser effect. *J. Am. Chem. Soc.* 94:2561.
6. SON, T.-D., and C. CHACHATY. 1973. Nucleoside conformations in aqueous solution by proton magnetic resonance spectroscopy. *Biochim. Biophys. Acta.* 335:1.
7. SON, T.-D., W. GUSCHLBAUER, and M. GUERON. 1972. Flexibility and conformations of guanosine monophosphates by the Overhauser effect. *J. Am. Chem. Soc.* 94:7903.
8. NOGGLE, J. H., and R. E. SCHIRMER. 1971. *The Nuclear Overhauser Effect. Chemical Applications.* Academic Press, Inc., New York and London. 92.
9. WOESSNER, D. E. 1962. Spin relaxation processes in a two-proton system undergoing anisotropic re-orientation. *J. Chem. Phys.* 36:1.
10. WOESSNER, D. E. 1965. Nuclear magnetic dipole-dipole relaxation in molecules with internal motion. *J. Chem. Phys.* 42:1855.
11. DODDRELL, D., V. GLUSHKO, and A. ALLERHAND. 1972. Theory of nuclear Overhauser enhancement and ¹³C-¹H dipolar relaxation in proton decoupled carbon-13 NMR spectra of macromolecules. *J. Chem. Phys.* 56:3683.
12. WERBELOW, L. G. 1974. Homonuclear Overhauser enhancements as probes of molecular mobility. *J. Am. Chem. Soc.* 96:4747.
13. ROWAN, R., J. A. MCCAMMON, and B. D. SYKES. 1974. A study of the distances obtained from nuclear magnetic resonance nuclear Overhauser effect and relaxation time measurements in organic structure determination. Distances involving internally-rotating methyl groups. Application to *cis*- and *trans*-crotonaldehyde. *J. Am. Chem. Soc.* 96:4773.
14. LEIGH, J. S., JR. 1968. A new technique for radio frequency magnetic field measurement. *Rev. Sci. Instrum.* 39:1594.
15. COULTER, C. L. 1973. Structural chemistry of cyclic nucleotides. II. Crystal and molecular structure of sodium β -cytidine 2',3'-cyclic phosphate. *J. Am. Chem. Soc.* 95:570.
16. SUNDARALINGAM, M. 1966. Stereochemistry of nucleic acid constituents. III. Crystal and molecular structure of adenosine 3'-phosphate dihydrate (adenylic acid b). *Acta Crystallogr.* 21:495.
17. KRAUT, J., and L. H. JENSEN. 1963. Refinement of the crystal structure of adenosine-5'-phosphate. *Acta Crystallogr.* 16:79.
18. WHITE, D. N. J. 1977. The principles and practice of molecular mechanics calculations. *Comp. Chem.* 1:225.
19. SCHIRMER, R. E., J. H. NOGGLE, J. P. DAVIS, and P. A. HART. 1970. Determination of molecular geometry by quantitative application of the nuclear Overhauser effect. *J. Am. Chem. Soc.* 92:3266.

20. LAVALLEE, D. K., and C. L. COULTER. 1973. Structural chemistry of cyclic nucleotides. III. Proton magnetic resonance studies of β -pyrimidine nucleotides. *J. Am. Chem. Soc.* **95**:576.
21. LAPPER, R. D., and I. C. P. SMITH. 1973. A ^{13}C and ^1H nuclear magnetic resonance study of the conformations of 2',3'-cyclic nucleotides. *J. Am. Chem. Soc.* **95**:2880.
22. COZZONE, P. J., and O. JARDETSKY. 1976. Phosphorus-31 Fourier transform nuclear magnetic resonance study of mononucleotides and dinucleotides. 2. Coupling constants. *Biochemistry*. **15**:4860.
23. SCHLEICH, R., B. P. CROSS, and I. C. P. SMITH. 1976. A conformational study of adenylyl-(3' \rightarrow 5')-adenosine and adenylyl-(2' \rightarrow 5')-adenosine in aqueous solution by carbon-13 magnetic resonance spectroscopy. *Nucleic Acids Research*. **3**:355.
24. HALL, L. D., and R. B. MALCOLM. 1972. Studies of organophosphorus derivatives. Part I. Nuclear magnetic resonance studies of the 2-oxo-1,3,2-dioxaphosphorinane system. *Can. J. Chem.* **50**:2092.
25. EVANS, F. E., and R. H. SARMA. 1974. The intramolecular conformation of adenosine 5'-monophosphate in aqueous solution as studied by fast Fourier transform ^1H and ^1H - ^{31}P nuclear magnetic resonance spectroscopy. *J. Biol. Chem.* **249**:4754.
26. SARMA, R. H., R. J. MYNOTT, D. J. WOOD, and F. E. HRUSKA. 1973. Determination of the preferred conformations constrained along the C-4'-C-5' and C-5'-O-5' bonds of β -5'-nucleotides in solution. Four-bond ^{31}P - ^1H coupling. *J. Am. Chem. Soc.* **95**:6457.
27. DAVIS, J. P., and P. A. HART. 1972. A nuclear Overhauser effect study of purine nucleoside glycosyl conformation in solution. *Tetrahedron*. **28**:2883.